Chemistry–A European Journal
Research Article
doi.org/10.1002/chem.202301508
Chemistry Europe
European Chemical Societies Publishing
www.chemeurj.org

Special Collection

EPR Sensing of a Cation Species by Aza-Crown Ethers Incorporating a Persistent Nitroxidic Radical Unit

Cecilia Poderi,[a] Iago Neira,[b] Paola Franchi,[a] Elisabetta Mezzina,[a] Ilario Baù,[a] Paolo Neviani,[a] and Marco Lucarini*[a]

Dedicated to Prof. Maurizio Prato in occasion of his retirement

New nitroxides based on aza-crown ethers were prepared and employed as selective sensors for the detection of inorganic and organic cations by EPR analysis of the corresponding host–guest complexes. The nitroxide unit behaves as a sensitive probe for a number of alkali and alkaline earth metal cations affording EPR spectra differing in the value of nitrogen hyperfine constants and in the appearance of splitted signals due to the non-zero nuclear spin of some metal cation upon complexation. Owing to the remarkable EPR spectral differences between the host and the corresponding cation complex the new macrocycles are likely to act as multitasking tools to recognize several cationic species. EPR behaviour of the larger nitroxide azacrown **1**• when acting as a wheel in a radical synthetic bistable [2]rotaxane containing both secondary dialkylammonium and 1,2-bis(pyridinium) molecular stations, was also investigated. Reversible movements of the macrocycle between the two recognition sites in the rotaxane were promptly revealed by EPR, which shows significant changes either in nitrogen coupling constant values (a_N) or in the spectral shape in the two rotaxane co-conformations.

Introduction

Crown ethers[1] have been widely applied as sensors for ions and molecular scaffolds in the design of materials and biological models[2] owing to strong binding with various metal ions and chemical species. As an example, suitable chemosensors for metal ions obtained covalently linking fluorophores to crown ether macrocycles afford a platform to monitor relevant biological process in vivo.[3]

An alternative approach consists in introducing radical probes as side substituent of a crown ether moiety. In these systems, EPR spectroscopy[4] acquires a key role in the detection and monitoring of binding events, association/dissociation processes, conformational and dynamic motions affecting the substrates, thanks to its high sensitivity to the chemical environment surrounding the paramagnetic units.[5]

Some years ago we reported the synthesis and the characterization of dialkyl nitroxide radicals bound through a methylene bridge to a dibenzo-24-crown-8-ether (DB24C8) group which were able to probe complexation of metal and organic cations by EPR spectroscopy.[6] In those assemblies we could prove that benzyl protons EPR hyperfine coupling constants were affected by binding in a measure depending on the nature of the cation guests, although the proposed nitroxide framework was characterized by a reduced lifetime if compared to sterically hindered nitroxides.[7]

An interesting development in the field of molecular machines (MIM) was the introduction of a stable nitroxide[7] radical (2,2,6,6-tetramethylpiperidine-1-oxyl, TEMPO) both in DB24C8 wheel and in the axle components of paramagnetic MIMs.[8] In these chemical assemblies the reversible shuttling motion of the paramagnetic wheel was investigated monitoring the distance between the two spin centers both by CW EPR spectroscopy and pulsed EPR tecniques.[8]

Possibility to extend spin probe methodology in azacrown ethers by oxidation of the nitrogen to a stable nitroxide macrocycle makes the radical behaving as a recognizing unit for the guest hosted inside. Nitroxyl groups (N–O•) are known to accept halogen and hydrogen bonds and in general to act as non-covalent interaction reporters.[9,10] Thus, the conversion of the inner nitrogen of an azacrown ether into a nitroxyl radical enables larger exposition to non-covalent interactions with included guests, potentially enhancing the complexing ability of these compounds. Their incorporation in crown ether structures could be a powerful tool for the preparation of novel

[a] Dr. C. Poderi, Prof. Dr. P. Franchi, Prof. Dr. E. Mezzina, Dr. I. Baù, Dr. P. Neviani, Prof. M. Lucarini
Department of Chemistry "Giacomo Ciamician"
University of Bologna
Via P. Gobetti 83, 40129 Bologna (Italy)
E-mail: marco.lucarini@unibo.it

[b] Dr. I. Neira
Departamento de Química
Centro Interdisciplinar de Química y Biología (CICA)
Universidade da Coruña, Facultad de Ciencias
Coruña, E-15071A (Spain)

Supporting information for this article is available on the WWW under https://doi.org/10.1002/chem.202301508

This article is part of a joint Special Collection in honor of Maurizio Prato.

multi-featured ionophores, to be used in the fields of biochemistry and radical molecular machinery.

This was recently achieved by inserting a dialkyl nitroxide functionality in a crown ether-like frame containing seven ethereal oxygen atoms (**C•**, Figure 1).[11] The shuttling process of the new paramagnetic wheel **C•** along a diamagnetic dumbbell composed of dialkylammonium and 4,4′-bipyridinium recognition sites, was also demonstrated by detecting a significant change of the nitrogen coupling constant in the EPR spectra after addition of a base to the rotaxane.[11]

In an effort to design new stable paramagnetic hosts we decided to further explore the use of aliphatic azacrown ether as spin probe precursor. In 1985, the synthesis of novel aliphatic monoazacrown macrocycles (**3•**, see Figure 1) containing 5 ethereal oxygen atoms was reported.[12] Complexation toward Na^+ and K^+ cations was also investigated by EPR. Quite surprisingly, the authors did not detect any EPR evidence of complexation. We decided to re-investigate in details the binding properties of this heterocycle family by preparing also novel larger member containing 6 and 7 oxygen atoms (**1•** and **2•**, see Figure 1). EPR spectroscopy was employed to study the host properties of the target ligands and to calculate the association equilibrium constants (K_a) of complexes formed with different inorganic and organic cationic guests.

In addition, nitroxide crown ether **1•** was tested as the wheel in a bistable [2]rotaxane, containing dialkylammonium and 4,4′-bipyridinium recognition sites.

Results and Discussion

Scheme 1 reports the synthetic steps to obtain the nitroxyl radical (**1•**) derived by tetramethyl-24-azacrown-7-O ether **1**. The azacrown was prepared adapting the procedure described by Lai and co-workers.[12]

In detail, 3,3,5,5-tetramethylmorpholin-2-one **5** was obtained by the multicomponent Bargellini reaction using amino-alcohol **4** with chloroform and acetone in NaOH solution. Aminodiol **6** was afforded after reduction of **5**.

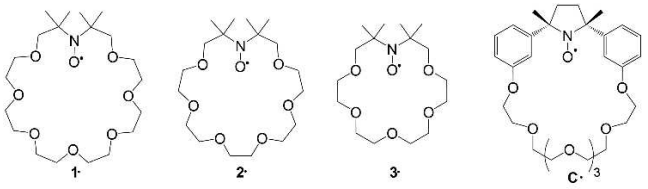

Figure 1. Molecular structures of the investigated nitroxyl crown ethers **1•**–**3•** and of the macrocycle **C•** described in Ref. [11].

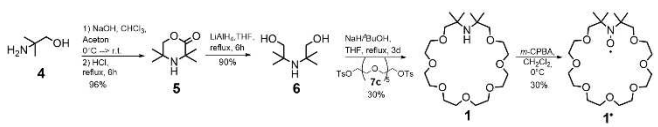

Scheme 1. Synthetic pathway of macrocycle **1•**.

The cyclization step was promoted by NaH/^{t}BuOH in the presence of a bis-tosylated glycol chain **7c**. Finally, oxidation of amine **1** to nitroxide was performed using 3-chloroperbenzoic acid (*m*-CPBA), and affording the final radical macrocycle (**1•**) in 30% yield. The low yield (30%) of the cyclic radical is due to a partial over-oxidation of the cyclic nitroxide to a nitroso-derivative with *m*-CPBA leading to the formation of a ring-opened bright blue by-product. The by-product (Scheme S2, Supporting Information) is prevailing in presence of an excess of peracid. To minimize the nitroso formation, we employed a smaller amount of peracid (0.7 eq) and followed the progressive formation of nitroxide **1•** by EPR, monitoring the signal intensity of the radical until a *plateau*. Thus, the reaction was quenched by addition of 1 equivalent of $Ba(OH)_2$ and purified by chromatography column.

Similar procedure was employed for the synthesis of **2•** and **3•** (see Supporting Information).

EPR studies

Metal cations with I = 0.

When Ca^{2+}, Mg^{2+}, Ba^{2+} or Sr^{2+} cations are added in acetonitrile (ACN) to ligands **1•**, **2•** or **3•**, generically indicated as **L•**, the corresponding EPR spectra show additional signals which were assigned to the complexed radical **L•**@M^{n+} in equilibrium with the free nitroxide (Scheme 2).

As an example, Figure 2 reports the spectral lines of free **1•** and **1•**@Ca^{2+} nitroxides displaying a difference of 1.5 G between the coupling constants values (a_N) of the two species in equilibrium in ACN. When the concentration of metal cations is increased until a threshold value that depends on the affinity of

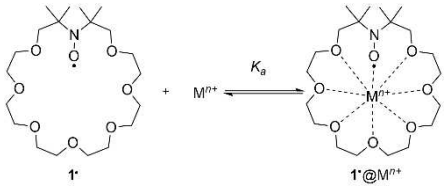

Scheme 2. Complexation equilibrium between **1•** and metal cation guest (M^{n+}).

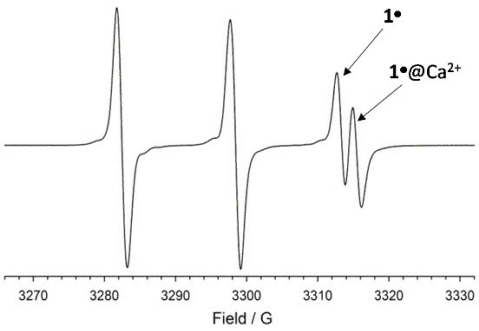

Figure 2. Spectrum EPR of **1•** (5×10^{-5} M) in acetonitrile (ACN) in the presence of calcium picrate 0.058 mM.

Table 1. EPR spectroscopic parameters of **1**•@M^{n+} and calculated K_a for the association between **1**• and different guests in acetonitrile,[a] acetonitrile/H_2O 99/1,[b] and acetone.[c]

Entry	Salt	Cation	K_a/M^{-1} (T = 294 K)	a_N/G	$a_M{}^{n+}$/G	Ionic radius (Å)	Cation Nuclear spin (*I*)
1	$LiClO_4$[a]	Li^+	536	16.05	1.37	0.76	3/2
2	$NaClO_4$[a,d]	Na^+	9000	15.45	2.53	1.02	3/2
3	Na picrate[a,d]	Na^+	9000	15.46	2.49	1.02	3/2
4	K picrate[a,e]	K^+	11000	15.52		1.38	0
5	$RbClO_4$[a,f]	$^{87}Rb^+$ (27.88%)	Not determined	15.65	4.81	1.52	3/2
		$^{85}Rb^+$ (72.12%)		15.59	1.41		5/2
6	Cs picrate[a]	Cs^+	5042	15.75	2.66	1.67	7/2
7	$Mg(ClO_4)_2$[a]	Mg^{2+}	2921	17.22		0.72	0
8	$Ca(picrate)_2$[a]	Ca^{2+}	59600	16.75		1.00	0
9	$Sr(picrate)_2$[a]	Sr^{2+}	100000	16.50		1.18	0
10	RbCl[b]	$^{87}Rb^+$ (27.88%)	6374	15.66	4.63	1.52	3/2
		$^{85}Rb^+$ (72.12%)		15.65	1.35		5/2
11	$Ba(CH_3COO)_2$[b]	Ba^{2+}	2405	16.28		1.35	0
12	NH_4PF_6[a]	$NH_4{}^+$	12334	15.88		1.4	0
13	$(PhCH_2)_2NH_2PF_6$[a]	$(PhCH_2)_2NH_2{}^+$	117	16.01			0
14	Na picrate[c]	Na^+	613	15.27	2.32	1.02	3/2
15	Cs picrate[c]	Cs^+	1570	15.76	2.63	1.67	7/2
16	$Ca(picrate)_2$[c]	Ca^{2+}	61	16.53		1.00	0
17	$(PhCH_2)_2NH_2PF_6$[c]	$(PhCH_2)_2NH_2{}^+$	21	16.04			0

[a] The hyperfine coupling constant (a_N) of **1**• is 15.24 G in acetonitrile. [b] The hyperfine coupling constant (a_N) of **1**• is 15.34 G in acetonitrile/H_2O 99:1. [c] The hyperfine coupling constant (a_N) of **1**• is 15.06 G in acetone. [d] Two different salts of the same cation were examined to prove that different anions do not affect complexation. [e] K_a was determined indirectly, by displacement of the Ca^{2+} from **1**•, as explained in the text. [f] $RbClO_4$ is almost insoluble in acetonitrile.

the metal examined for the macrocycle, the spectrum of the radical crown binding the cation, **1**•@M^{n+}, becomes dominant allowing the measurement of the spectroscopic parameters of the bound nitroxide (see Table 1).

The increase of a_N is a clear indication that presence of the metal induces a rather remarkable gain in the odd-electron (spin) population at the nitrogen center. At the same time, the *g*-factor shows an opposite trend, decreasing when passing from the free to the complexed nitroxide. Since the hyperfine splittings and *g*-factors of EPR spectra are known to be sensitive to environmental perturbations, the reported behaviour is expected for nitroxide molecules forming a coordination complex with a metal cation in close contact with the oxygen atom of the nitroxide group.

The metal cation acting as a Lewis acid site causes a shift of charge towards the oxygen atom and consequently a shift of spin density towards the nitrogen atom (see Scheme 3). As expected, this behaviour is more pronounced in the case of dication guests or smaller monocations.

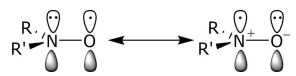

Scheme 3. Resonance structures of dialkyl nitroxide radicals.

Metal cations with $I \neq 0$.

In addition to the increase of a_N, complexation of metal cations with non-zero nuclear spins ($^{133}Cs^+$, $^{23}Na^+$ and $^{7}Li^+$) also produces line splitting deriving from the coupling of the unpaired electron of **1**• with the complexed spin active nuclei, $a_M{}^{n+}$, according to the relationship $N_{lines} = (2n_A I_A + 1)(2n_B I_B + 1)\ldots(2n_N I_N + 1)$. Moreover, complexation of metal cations of different isotopic forms, as in the case of $^{85}Rb^+$ and $^{87}Rb^+$, resulted in an EPR spectrum reflecting the interaction of the unpaired electron with both isotopes of Rb cations and enabling to distinguish each isotopic contribution. For example, Figure 3 shows some experimental spectra and the relative theoretical simulation.

Calculated equilibrium association constants (K_a) of L•@M^{n+} by EPR measurements

The analysis was carried out using constant concentrations of **L**• (0.5–1.0×10^{-4} M) in the presence of variable amounts of each guest, and extrapolating the ratio between the concentrations of bound and free form of **L**• $\left(\frac{[L\cdot@M^{n+}]}{[L\cdot]}\right)$ by using EPR spectra simulation. The K_a values were obtained considering the angular coefficient of the linear regression plots reporting the calculated

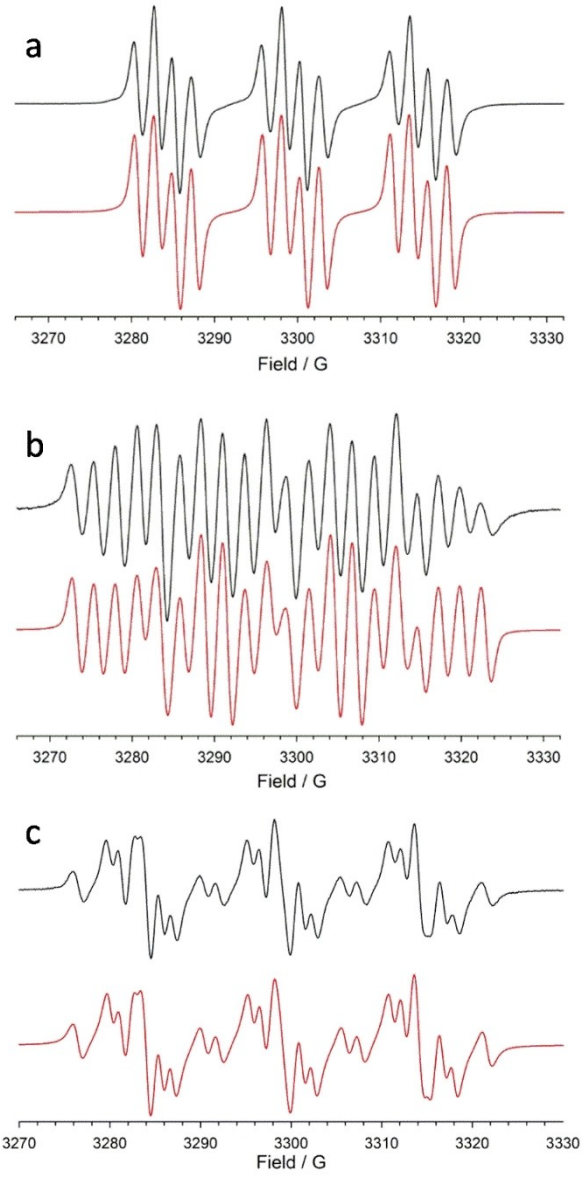

Figure 3. EPR spectra of **1•** (5×10^{-5} M) in ACN at 298 K in the presence of a) 1.0 mM of $NaClO_4$ (^{23}Na, I = 3/2, 100%), b) 2.5 mM of Cs picrate, (^{133}Cs, I = 7/2, 100%), c) traces of $RbClO_4$ (^{85}Rb, I = 5/2, 72%, ^{87}Rb, I = 3/2, 28%). The corresponding theoretical simulations (in red) are obtained by employing the spectroscopic parameters of Table 1.

values of $\frac{[L^{\cdot}@M^{n+}]}{[L^{\cdot}]}$ as a function of guest concentration. In the presence of a large excess of guest, the value of K_a was approximated according to the following equation:

$$K_a = \frac{[\boldsymbol{L}^{\cdot}@M^{n+}]}{[\boldsymbol{L}^{\cdot}][M^{n+}]} = \frac{[\boldsymbol{L}^{\cdot}@M^{n+}]}{[\boldsymbol{L}^{\cdot}][M^{n+}]_0} \quad (1)$$

Alternatively, when using concentrations of guest comparable to those of **1•**, the K_a were obtained considering the complete mathematical treatment (see Supporting Information).

Concerning the complexation of K^+ cation, for which no significant spectral variations were observed in the presence of ligand **1•**, the K_{K^+} was indirectly calculated thanks to competitive titrations performed by adding different concentrations of a K^+ salt to samples containing known and fixed amounts of macrocycle **1•** and Ca^{2+}. (see Supporting Information)

Results obtained for 1•@M^{n+} by EPR measurements

Data of Table 1 have been obtained by measuring sufficiently intense signals of free and complexed species in concentrations of host macrocycle and cations up to 1×10^{-7} M and 2×10^{-6} M in acetonitrile (ACN), respectively.

More specifically, data reported in Table 1 show that the association constants K_a of **1•** increases with the ionic radius of the guest in the series Li^+, Na^+ and K^+ (Entries 1–4); Mg^{2+} Ca^{2+} and Sr^{2+}, (Entries 7–9) and, for cations of the same size, with the charge density (i.e. Na^+ vs Ca^{2+}, Entries 2 and 8). An exception was noticed for K^+ cation (Entry 4), in which the corresponding K_{K^+} was estimated over twice larger than K_{Cs^+} (Entry 6). In this case we suppose that the conformation adopted by **1•** is more favourable when binding K^+ than Cs^+.

It is important to note that the affinities of the alkali cations for **1•** are very similar to the reported values in ACN for the closely related diamagnetic macrocycle dibenzo[24]crown-8 (i.e. with Na^+ $K_a = 12590\ M^{-1}$, K^+ ($K_a = 6310\ M^{-1}$).[13]

This suggests that the presence of the nitroxide unit does not reduce the complexing capacity of the crown ether moiety.

In order to complete the analysis of the complexation of alkaline and alkaline-earth metal cations, supplementary experiments in ACN/H_2O 99/1 were performed using salts not soluble in pure acetonitrile, i.e. RbCl and $Ba(CH_3COO)_2$, (Entries 10 and 11), for which the obtained affinities values reflect the cation-diameter-hole-size relationship.

In addition, the affinity of organic dibenzylammonium cation (DBA) in ACN was found significantly lower than that obtained by the corresponding inorganic NH_4^+ (Entry 13 vs. 12), but sufficiently high to propose the synthesized macrocycle **1•** as a wheel of a multi-station rotaxane, including one based on the DBA.

Entries 14–17 report the binding constants of some salts obtained in acetone. In general, we observe a sensitive decrease of the values relatively to those measured in ACN for the same cations, presumably because the solvation enthalpies and entropies of the cations and ligand are unfavourable to complexation. Calcium dication feels the solvent change even more, displaying a dramatic inhibition to the complexation (compare entries 8 and 16), probably because of the larger charge density which results in a more efficiently solvation in acetone than in acetonitrile.

Table 2. EPR spectroscopic parameters and calculated K_a for the complexation between **2•**[a] or **3•** [a] and selected guests in ACN.[b]

Salt	Cation (I_N)	Crown ether **2•** K_a/M^{-1} (T = 294 K)	Crown ether **3•** K_a/M^{-1} (T = 294 K)	a_N/G **2•**	$a_M{}^{n+}$/G **2•**	a_N/G **3•**	$a_M{}^{n+}$/G **3•**	Ionic radius (Å)
$LiClO_4$	Li^+ (3/2)	1381	1219	16.20	1.14	16.25	1.97	0.76
$NaClO_4$	Na^+ (3/2)	22656	41630	15.48	2.68	15.99	2.30	1.02
K picrate	K^+ (0)	26398	58603	15.70	/	16.26	/	1.38
Cs picrate	Cs^+ (7/2)	–	3346	–	–	16.54	3.29	1.67
$Mg(ClO_4)_2$	Mg^{2+}(0)	14059	–	17.42	/	–		0.72
$Ca(picrate)_2$	Ca^{2+} (0)	53208	59370	16.81	/	16.70	/	1.00
$Sr(picrate)_2$	Sr^{2+} (0)	94660[c]	–	16.32	/	–		1.18

[a] [**2•**] = [**3•**] = 4–8×10^{-5} M. [b] The hyperfine coupling constants (a_N) in ACN of **2•** and **3•** are 15.36 and 15.42 G, respectively. [c] This value refers to the formation of a 1:2 complex between Sr^{2+} cation and two crown ether **2•** molecules.

Results obtained for 2•@M^{n+} and of 3•@M^{n+} by EPR measurements

Table 2 reports the estimated complexation parameters of selected cations in ACN using smaller sized radical macrocycles **2•** and **3•**, synthesized in the present study, in order to evaluate the host fitting of the metal guest. In general, spectral behavior of radicals **2•** and **3•** towards examined metals resembles that already observed in **1•**@M^{n+} complexes: once again the spectral lines of free and bound crown nitroxides display a difference in the a_N value and in the splitting of signals in the case of metal cation with non-zero nuclear spin. The increase of a_N value is more evident in the case of small and dications species (i.e. **2•**@Mg^{2+}). However, a high value of a_N is observed also in the case of complexes of **3•** with alkaline low charge density Cs^+ and K^+ cations; in this case a closer distance between the complexed ion and nitroxide function in smaller macrocycle may justify the obtained large a_N value.

For what concerns the relationship between the ionic radius size and the association constants of the three ligands, Figure 4 further summarizes the obtained results in graphic form.

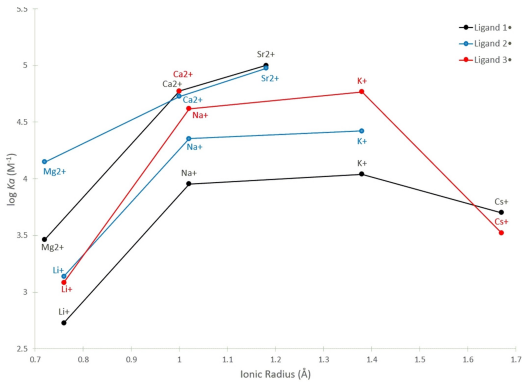

Figure 4. Graphical representation of the relationship between the ionic radius of the metal cations examined and the logK_a of the three proposed ligands. The black, blue, and red lines and dots refer to the results found for macrocycle **1•**, macrocycle **2•**, and macrocycle **3•**, respectively.

In analogy with literature data[14] obtained by potentiometric techniques for conventional crown ethers, Na^+ and K^+ cations proportionally increase their affinity towards the smaller paramagnetic macrocycles, which become more suited to accommodate them. In line with these results, the small Li^+ forms complexes with radicals **2•** and **3•** of similar stability, however relatively low compared to the other cations considered, while the affinity values halves when the host is the largest macrocycle **1•**. On the other hand, the large Cs^+ is best fitted in **1•** than in the smaller sized **2•** and **3•**. Large and very similar K_a values are calculated in complexes of all the radical macrocycles with Ca^{2+} ion.

This result might be explained in terms of similar peculiar electrostatic interactions that occur between the calcium ion and the nitroxide function in the various macrocycles, regardless of the number and proximity of the ether oxygen donors present in the different crowns. Finally, a complex having a metal to ligand ratios of 1:2 between Sr^{2+} and macrocycle **2•** could be proposed on the basis of the irregular variation of the ratio between the bound and free form of the radical in function of the cation concentration (see Supporting Information). In this case a "sandwich" structure in which the metal ion is located between two crown radical molecule is suggested.[15]

It is worth noting that the designed host systems are so sensitive that the presence of different metal ions in the same sample can be detected in the EPR spectrum by the appearance of distinct signals for each formed coordination complex. The relative amounts of the single species can be calculated by simulating the experimental spectrum using Equation (1) and the determined association constant values of each complex. As an example, Figure 5 shows the spectrum of macrocycle **3•** in ACN in presence of Cs^+ and Na^+, along with the related theoretical simulation that made possible to identify and quantify both cations.

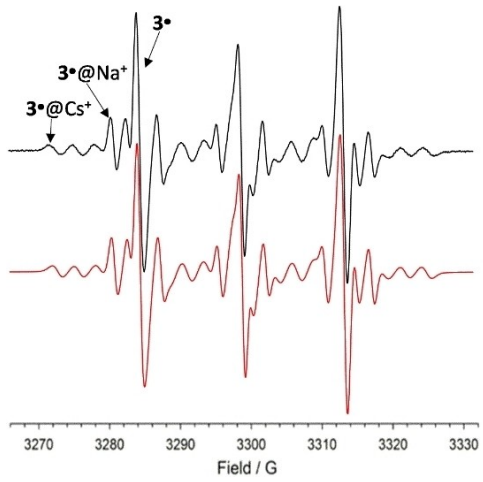

Figure 5. EPR spectra of **3•** (5×10^{-5} M) in ACN in the presence of $NaClO_4$ 0.024 mM and Cs picrate 0.28 mM, as derived from the theoretical simulation (in red) obtained by employing the spectroscopic parameters reported in Table 2 and the following relative percentages of the present species: **3•**@Na^+ = 34%, **3•**@Cs^+ = 32%, **3•** = 34%.

Calculated association constants (K_a) of 1•@M^{n+}, 2•@M^{n+} and 3•@M^{n+} in acetonitrile/H_2O mixtures by EPR measurements

Given the sensitivity of the method developed and the results obtained in organic solvent, we evaluated whether the complexing properties of the new radical ligands were maintained increasing the water content of the organic solution of salts. Table 3 shows the results obtained in the presence of some representative cations in ACN/H_2O mixtures (Further results are reported in the Supporting Information). In order to increase the range of cationic concentrations that can be studied and assess how the polarity of the medium affects the complexation process, mixtures starting from ACN/H_2O 99/1 (*i.e.* 1–100 mg/L) was employed, and subsequently higher water content and higher concentrations of cations were explored (i.e. 50–500 mg/L for ACN/H_2O 95/5, and >500 mg/L for ACN/H_2O 90/10).[16] Spectroscopic parameters of free and occupied radical ligands remain significantly distinct in the mixtures tested and the simulation of the obtained spectra allows their quantification. The results indicate that the proposed macrocycles still preserve the capacity to capture cations. In comparison to what is seen in pure ACN, the presence of 1% H_2O causes a small but significant decrease of the affinity of Mg^{2+} for macrocycle **1•**, whereas a more contained reduction in the Na^+ association constant with macrocycles **2•** and **3•** is observed. Also in these conditions the three ligands show the same affinity toward Ca^{2+} ions, which is about one third of that observed in acetonitrile while the affinity of Na^+ for the three macrocycles continues to decrease proportionally and slowly as the percentage of water present increases, remaining surprisingly high, for the tested macrocycle **2•**, even when water is added up to 10%. The K^+ appears to follow a similar behavior with macrocycle **3•**. In contrast, the affinity of Ca^{2+} swiftly

Table 3. EPR spectroscopic parameters and calculated K_a for the association between **1•**, **2•** and **3•** and different cations[a] in mixtures ACN/H_2O.[b]

Cation[b]	Mixture ACN/H_2O	Crown ether **1•** K_a/M^{-1}	Crown ether **2•** K_a/M^{-1}	Crown ether **3•** K_a/M^{-1}	*a*/G **1•** bound	*a*/G **2•** bound	*a*/G **3•** bound
Na^+ ($I=3/2$) ($r=1.02$ Å)	99/1	765	5116	11215	$a_N=15.46$ $a_{Na^+}=2.38$	$a_N=15.45$ $a_{Na^+}=2.60$	$a_N=16.09$ $a_{Na^+}=2.10$
K^+ ($I=0$) ($r=1.38$ Å)	99/1			8975			$a_N=16.26$
Mg^{2+} ($I=0$) ($r=0.72$ Å)	99/1	270	467	1850	$a_N=16.74$	$a_N=16.87$	$a_N=16.76$
Ca^{2+} ($I=0$) ($r=1.00$ Å)	99/1	18985	17776	19818	$a_N=16.78$	$a_N=16.82$	$a_N=16.70$
Na^+ ($I=3/2$) ($r=1.02$ Å)	95/5	135	539	2108	$a_N=15.68$ $a_{Na^+}=2.11$	$a_N=15.63$ $a_{Na^+}=2.31$	$a_N=16.08$ $a_{Na^+}=1.98$
K^+ ($I=0$) ($r=1.38$ Å)	95/5			2597			$a_N=16.34$
Ca^{2+} ($I=0$) ($r=1.00$ Å)	95/5	219		618	$a_N=16.53$		$a_N=16.69$
Na^+ ($I=3/2$) ($r=1.02$ Å)	90/10		294			$a_N=15.66$ $a_{Na^+}=2.10$	

[a] Two different salts (chlorides and perchlorates) of the same cation were examined, obtaining the same results. [b] The hyperfine coupling constants (a_N) of **1•**, **2•** and **3•** are 15.34 G, 15.45 G and 15.50 G in ACN/H_2O 99:1, respectively. The hyperfine coupling constants (a_N) of **1•**, **2•** and **3•** are 15.48 G, 15.57 G and 15.65 G in ACN/H_2O 95:5, respectively. The hyperfine coupling constants (a_N) of **3•** is 15.72 G, in ACN/H_2O 90:10

decreases when the water content of the mixture rises, this time more dramatically for macrocycle **1•** than for **3•**.

We can conclude that the proposed ligands are so sensitive that, even when dissolved in mixtures containing small amounts of water, they can still sense the presence of different metal cations in a single sample, producing separate signals for each generated complex that are identifiable and quantifiable after spectral simulation.

Synthesis and shuttling of a radical molecular machine based on 1•

In order to investigate the possible applications of **1•** in the field of radical MIMs, its complexing behaviour was applied also to the organic dibenzylammonium cation (DBA), which represents a recognition station present in many linear components of rotaxanes.[11] Actually, the EPR spectrum of **1•** shows a significant increase of a_N constant after DBA salt addition (from 15.24 to 16.01 G, Table 1) (Figure 6a), indicating a considerable affinity of the macrocycle towards this organic species. In addition, the spectral shape of the complex changes too, leading to an apparent broadening of the external lines as a consequence of the increased rotational correlation time of the complex. Similar variations are detected when the dication half thread (**8H**$^{2+}$) precursor of many bistable rotaxane structures, is hosted by the radical macrocycle (Figure 6b). Thanks to these spectral features we decided to undertake the synthesis of [2]rotaxane **RH**$^{\bullet 3+}$ (Scheme 4) containing dialkylammonium and 4,4′-bipyridinium recognition sites. The MIM was assembled by applying the well known *threading-stoppering* approach which consists in the formation of the pseudorotaxane (**1•@8H**$^{2+}$), and in the subsequent trapping with 3,5-di-^{t}butylbenzylbromide in methylene chloride.[11] As described above evidence of threading of the dicationic rod into the radical macrocycle was detected following a_N coupling constant increase by EPR. In detail, adding discrete amounts of **8H**$^{2+}$ (up to 1.5 eq) to a known concentration solution of **1•** in CH_2Cl_2, we monitored the shift of EPR spectrum lines until reaching of a constant value. Once formation of **1•@8H**^{2} was complete, the stopper was added and the reaction refluxed for 5 days (see Supporting Information). **RH**$^{\bullet 3+}$ was isolated with a not yet optimized yield of 20% after chromatographic separation.

The rotaxane structure was confirmed by ESI-MS (see Supporting Information) and EPR spectroscopy. [17]

Figure 7 (red line) shows the EPR spectrum of rotaxane **RH**$^{\bullet 3+}$ recorded in acetonitrile at 298 K, exhibiting typical nitroxide EPR signals with the high field line broadening due to restricted tumbling. The value of $a_N = 16.08$ G is sensitively larger than that observed for the free macrocycle (15.24 G), indicating a specific non-covalent interaction between macrocycle N–O• and the ammonium station of the dumbbell. This feature, which is correlated to the spin density modification on the nitrogen atom and the minor conformational degree of the radical due to complexation, confirm the solution structure of the rotaxane. An in-depth EPR analysis of free and complexed macrocycle consisted in decreasing amplitude modulation (AM) in order to acquire more resolved spectra. In this case, the low field line of the rotaxane displays a further splitting due to the coupling of the unpaired electron with γ-protons (Figure 7b) which is not detected in the free macrocycle (Figure 7a).

Also base-induced movement of the macrocycle towards the bis-pyridinium station (Scheme 4) was followed by acquiring EPR spectra. Addition of increasing amounts of *i*-Pr_2EtN (DIPEA) to the rotaxane solution produces an increase in the EPR nitrogen coupling value of 0.2 G. Furthermore, more resolved spectral EPR (modulation amplitude 0.1 mT) of the two MIM co-conformations revealed distinct splitting patterns (Figure 8, spectra *a* and *b*),

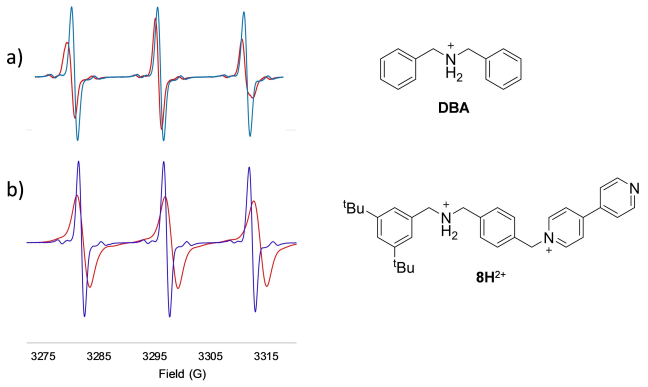

Figure 6. Comparison of the EPR spectra in acetonitrile of **1•** (blue line) and a) **1•** after addition of excess of DBA (red line); b) **1•** after addition of excess of **8H**$^{2+}$ (red line) indicating hosting of the organic cations.

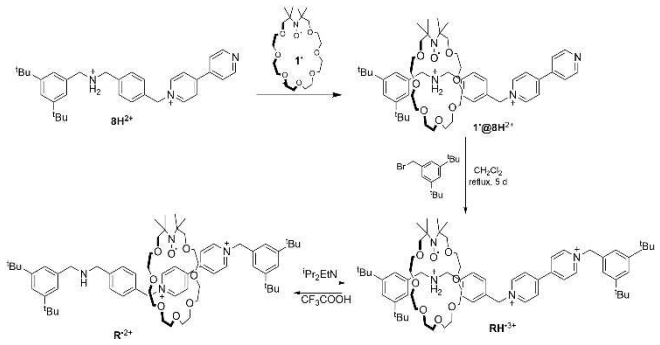

Scheme 4. Reaction scheme for the preparation of the rotaxane **RH**$^{\bullet 3+}$ and switching process between **RH**$^{\bullet 3+}$ and **R**$^{\bullet 2+}$.

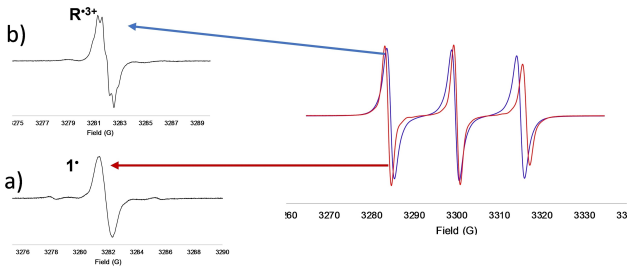

Figure 7. In the right side EPR spectra (amplitude modulation 1 mT) of macrocycle **1•** (blue line) and rotaxanes **RH**$^{\bullet 3+}$ (red line) in ACN at room T and in the left side insets displaying the low field line measured at amplitude modulation 0.1 mT of a) radical crown ether **1•**; b) rotaxane **RH**$^{\bullet 3+}$.

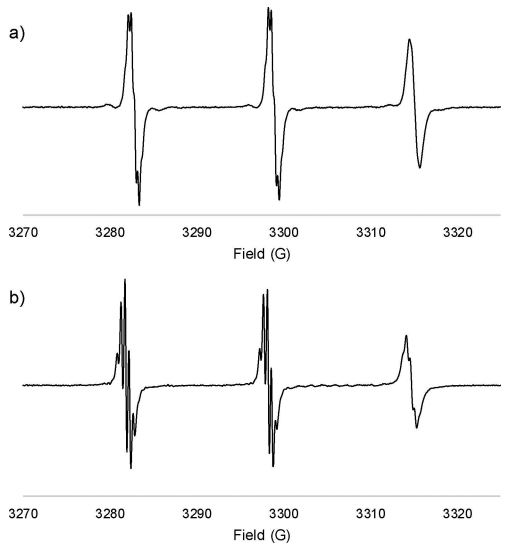

Figure 8. EPR spectra in ACN a 298 K of a) $\mathbf{RH^{\bullet 3+}}$; b) $\mathbf{RH^{\bullet 3+}}$ in the presence of DIPEA (3 eq).

In principle, the variation of the coupling constant could simply be due to the deprotonation of the ammonium site and the consequent complexation of the secondary amino group. However, this possibility was rejected for the following reasons:

i) we expect that the complexation of a neutral group results in a decrease of the nitrogen coupling constant and not in its increase as experimentally observed;
ii) no EPR spectral changes were observed on mixing the dibenzylamine model compound with the macrocycle.

On these bases, the observed spectral variation were attributed to the translational movement of the macrocycle along the dumbbell.

The subsequent addition of a stoichiometric amount of trifluoroacetic acid (TFA) to the same solution caused the quantitative recovery of the initial EPR spectrum as a consequence of the macrocycle returning to the preferred ammonium station (see Supporting Information).

Conclusions

In summary, the inclusion properties of paramagnetic aza-crown ether macrocycles $\mathbf{1^{\bullet}}$–$\mathbf{3^{\bullet}}$ towards alkaline, alkaline earth metals and few organic guests were tested. Evidence of the complexation was provided by remarkable changes of the spectral parameters (multiplicity and hyperfine constants) comparing the EPR spectra of the associated and non-associated forms. Thanks to these spectroscopic features, the association equilibrium constants (K_a), were calculated by theoretical simulations of the EPR spectra. The novel macrocycles showed a large affinity towards a variety of guest inorganic cations, as well as an excellent ability to distinguish them when present simultaneously, either in pure acetonitrile or acetonitrile-water mixtures. For these reasons, they could be suitable for the identification, measurement, extraction, and/or transport of cations in organic and mixed matrices.

Use of the largest radical macrocycle $\mathbf{1^{\bullet}}$ in the formation of radical MIMs allowed to obtain a [2]rotaxane, whose dumbbell includes ammonium and bis-pyridinium stations. In the molecular machine, pH change produces the typical reversible translational forth and back movement, which was quickly monitored by EPR without an appreciable loss of signal. This favourable feature in combination with the presence of redox-active persistent nitroxide radical makes the proposed rotaxane a suitable candidate for preparing molecular machines able to perform repetitive back and forth motion triggered by a catalytic oxidation cycle, which is maintained until a fuel is present.

Supporting Information

The authors have cited additional references within the Supporting Information (Ref. [18–20]).

Acknowledgements

This research was supported by the Italian Ministry of University Research through the projects PRIN2017 "BacHounds: Supramolecular nanostructures for bacteria detection" (2017E44A9P to ML and EM) and "Nemo" (20173L7W8K to PF).

Conflict of Interests

The authors declare no conflict of interest.

Data Availability Statement

The data that support the findings of this study are available in the supplementary material of this article.

Keywords: EPR spectroscopy · nitroxides · crown ether · cation · rotaxane

[1] C. J. Pedersen, *J. Am. Chem. Soc.* **1967**, *89*, 7017.
[2] G. W. Gokel, W. M. Leevy, M. E. Weber, *Chem. Rev.* **2004**, *104*, 2723.
[3] J. Li, D. Yim, W.-D. Jang, J. Yoon, *Chem. Soc. Rev.* **2017**, *46*, 2437.
[4] *Electron Paramagnetic Resonance: a practitioner's toolkit*, (Eds.: M. Brustolon, E. Giamello), John Wiley & Sons Inc., Hoboken, **2009**, 2995.
[5] Selected examples and reviews a) E. G. Bagryanskaya, S. R. A. Marque, *Electron Paramagn. Reson.* **2017**, *25*, 180; b) E. Mezzina, R. Manoni, F. Romano, M. Lucarini, *Asian J. Org. Chem.* **2015**, *4*, 296; c) M. Lucarini, *Encyclopedia of Radicals in Chemistry, Biology and Materials, Vol. 1* (Eds.: C. Chatgilialoglu, A. Studer), Wiley, Chichester, **2012**, pp. 229–248; d) D. Bardelang, M. Hardy, O. Ouari, P. Tordo, *Encyclopedia of Radicals in Chemistry, Biology and Materials, Vol. 4* (Eds.: C. Chatgilialoglu, A. Studer, Wiley, Chichester, **2012**, pp. 1965–2016; e) M. Lucarini, E. Mezzina, *Electron Paramagn. Reson.* **2010**, *22*, 41; f) M. Lucarini, *Eur. J. Org. Chem.* **2020**, *2995*; g) L. Gualandi, P. Franchi, E. Mezzina, S. M. Goldup, M. Lucarini, *Chem. Sci.* **2021**, *12*, 8385.

[6] L. Gualandi, P. Franchi, A. Credi, E. Mezzina and M. Lucarini, *Phys. Chem. Chem. Phys.* **2019**, *21*, 3558.
[7] G. I. Likhtenshtein, J. Yamauchi, S. Nakatsuji, A. I. Smirnov, R. Tamura, *Nitroxides: Applications in Chemistry, Biomedicine and Materials Science*, Wiley-VCH, Weinheim, **2008**.
[8] a) G. Jeschke, A. Godt, *ChemPhysChem* **2003**, *4*, 1328; b) V. Bleve, C. Schäfer, P. Franchi, S. Silvi, E. Mezzina, A. Credi, M. Lucarini, *ChemistryOpen* **2015**, *4*, 18; c) P. Franchi, V. Bleve, E. Mezzina, C. Schäfer, G. Ragazzon, M. Albertini, D. Carbonera, A. Credi, M. Di Valentin, M. Lucarini, *Chem. Eur. J.* **2016**, *22*, 8745; d) M.-E. Boulon, A. Fernandez, E. M. Pineda, N. F. Chilton, G. Timco, A. J. Fielding, R. E. P. Winpenny, *Angew. Chem. Int. Ed.* **2017**, *56*, 3876.
[9] a) R. Improta, V. Barone, *Chem. Rev.* **2004**, *104*, 1231;b) P. Franchi, M. Lucarini, P. Pedrielli, G. F. Pedulli, *ChemPhysChem.* **2002**, *3*, 789.
[10] a) L. Gualandi, E. Mezzina, P. Franchi, M. Lucarini, *Chem. Eur. J.* **2016**, *22*, 16017; b) G. R. Hanson, P. Jensen, J. McMurtrie, L. Rintoul, A. S. Micallef, *Chem. Eur. J.* **2009**, *15*, 4156.
[11] V. Bleve, P. Franchi, E. Konstanteli, L. Gualandi, S. M. Goldup, E. Mezzina, M. Lucarini, *Chem. Eur. J.* **2018**, *24*, 1198.
[12] a) J. T. Lai, *Synthesis* **1984**, 122; b) J. T. Lai, *J. Org. Chem.* **1985**, *50*, 1329.
[13] Y. Takeda, *Bull. Chem. Soc. Jpn.* **1983**, *56*, 3600.
[14] G. W. Gokel, D. M. Goli, C. Minganti, L. Echegoyen, *J. Am. Chem. Soc.* **1983**, *105*, 6786.
[15] R. M. Izatt, J. S. Bradshaw, S. A. Nielsen, J. D. Lamb, J. J. Christensen, D. Sen, *Chem. Rev.* **1985**, *85*, 271.
[16] For each cation, two different salts were used in each survey: chlorides, which are more common, but soluble in the mixtures under consideration only below a specific concentration; and perchlorates, which are less common, but completely soluble in the considered combinations. The association constants of the macrocycles investigated were measured and identical values were found in both instances, proving the validity of the experimental setup.
[17] As proof of the formation of rotaxane, the addition of concentrated Na^+ cation ([Na picrate] up to 12 mM) to a solution of the prepared structure, causes no change in the EPR spectrum, suggesting that the macrocycle is not accessible to metal cations, because its cavity is occupied by the cationic organic thread that is locked inside.

Manuscript received: May 12, 2023
Accepted manuscript online: July 12, 2023
Version of record online: ■■, ■■

RESEARCH ARTICLE

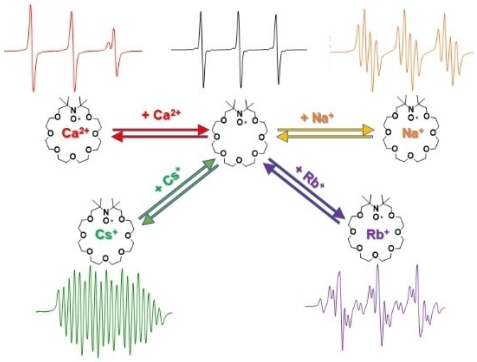

*Dr. C. Poderi, Dr. I. Neira, Prof. Dr. P. Franchi, Prof. Dr. E. Mezzina, Dr. I. Baù, Dr. P. Neviani, Prof. M. Lucarini**

1 – 10

EPR Sensing of a Cation Species by Aza-Crown Ethers Incorporating a Persistent Nitroxidic Radical Unit

The synthesis and the use of aza-crown ethers containing a stable nitroxide acting as selective sensor of inorganic and organic cations is described. The radical is deeply involved in the coordination complex generating peculiar EPR spectral pattern also depending on non-zero nuclear spin of the metal cation. The wheel was employed also in the preparation of a rotaxane structure.